

Unveiling the Origin of Fast Radio Bursts by Optical Follow Up Observations

Yuu NIINO¹ Tomonori TOTANI^{2,3} and Jun E. OKUMURA^{2,4}

¹*Division of Optical and IR Astronomy, National Astronomical Observatory of Japan, 2-21-1 Osawa, Mitaka, Tokyo
yuu.niino@nao.ac.jp*

²*Department of Astronomy, School of Science, The University of Tokyo, 7-3-1 Hongo, Bunkyo-ku, Tokyo*

³*Research Center for the Early Universe, School of Science, The University of Tokyo, 7-3-1 Hongo, Bunkyo-ku, Tokyo*

⁴*Department of Astronomy, Kyoto University, Kitashirakawa-Oiwakecho, Sakyo-ku, Kyoto*

(Received ; accepted)

Abstract

We discuss how we can detect and identify counterparts of fast radio bursts (FRBs) in future optical follow up observations of FRBs if real-time alert of FRBs becomes available. We consider kilonovae as candidates of FRB optical counterparts, as expected in the case that FRBs originate from mergers of double neutron star binaries. Although theoretical predictions on luminosities of kilonovae are still highly uncertain, recent models suggest that kilonovae can be detected at redshifts up to $z \sim 0.3$ within the range of the uncertainties. We expect ~ 1 – 5 unrelated supernovae (SNe) down to a similar variability magnitude in 5 days interval within the typical error radius of a FRB. We show that, however, a kilonova can be distinguished from these SNe by its rapid decay and/or color evolution, making it possible to verify the existence of a kilonova associated with a FRB. We also discuss the case that SNe Ia are FRB optical counterparts, as it might be if FRBs originate from double white dwarf binaries. Verification of this scenario is also possible, since the chance probability of finding a SNe Ia having consistent explosion time with that of a FRB within the FRB error region is small (typically $\lesssim 0.01$).

Key words: radio continuum: general — supernovae: general — stars: neutron — binaries: general

1. Introduction

Fast Radio Bursts (FRBs) are transient events recently discovered at \sim GHz frequency (Lorimer et al. 2007; Keane, Stappers, Kramer, & Lyne 2012; Thornton et al. 2013; Spitler et al. 2014). FRBs have typical durations of several milliseconds. Their large dispersion measures (DMs) suggest that FRBs are at cosmological distances corresponding to $z \sim 0.3$ – 1 .

Some models of the origin of FRBs were proposed recently, including merger of double neutron star binaries (NS-NS, Totani 2013), merger of double white dwarf binaries (WD-WD, Kashiyama, Ioka, & Mészáros 2013), hyperflares of magnetars (Popov & Postnov 2013), collapse of rotating super-massive neutron stars to black holes (Falcke & Rezzolla 2014; Zhang 2014), galactic flaring stars (Loeb, Shvartzvald, & Maoz 2014, but see also Tuntsov 2014; Dennison 2014), galactic exotic compact objects (Keane, Stappers, Kramer, & Lyne 2012; Bannister & Madsen 2014), and Perytons (Burke-Spolaor et al. 2011; Kulkarni et al. 2014).

The current localization errors of the FRBs are too large to identify host galaxies (or galactic progenitors) of FRBs. Discovery of FRB counterparts in other wavelengths is important to unveil the origin of FRBs. The currently known FRBs have been found in post analyses of pulsar survey data, and hence no follow up observation could be performed at the time of the bursts. Real-time alert and triggered multi-wavelength follow up observations are

desirable to improve our understanding on FRBs.

Some of the proposed FRB models predict the existence of counterparts in other wavelengths (e.g. Yi, Gao, & Zhang 2014). In the context of future FRB follow up observations in optical/near-infrared (NIR) wavelengths, the cases that a FRB results from a NS-NS or WD-WD merger, are particularly interesting. It is expected that NS-NS mergers cause a couple of transient events other than FRBs, namely short gamma-ray bursts (GRBs) and kilonovae. A kilonova is a transient event in optical/NIR powered by decay of radioactive elements formed via r -process nucleosynthesis in ejecta from a NS-NS merger.

The existence of kilonovae has been theoretically predicted (Li & Paczyński 1998), and a kilonova candidate was recently discovered in follow up observations of short GRB 130603B (Tanvir et al. 2013; Berger, Fong, & Chornock 2013). Kilonova emission lasts for a duration of days to weeks. Furthermore, kilonova emission is isotropic, and hence we would be able to detect it from every NS-NS merger that is close enough, unlike short GRBs that are most likely beamed. In this letter, we investigate how we can detect and distinguish kilonovae in future optical follow up observations of FRBs in the case that FRBs originate from NS-NS mergers.

We also briefly discuss the case that FRBs originate from WD-WD mergers. WD-WD mergers are promising candidates of the origin of type Ia supernovae (SNe Ia), although there are also other promising candidates (see Maoz, Mannucci, & Nelemans 2013 for a recent review).

If a SN Ia is associated with a FRB, it will be a good target of optical follow up observations (Kashiyama, Ioka, & Mészáros 2013).

Throughout this letter, we assume the fiducial cosmology with $\Omega_\Lambda = 0.7$, $\Omega_m = 0.3$, and $H_0 = 70 \text{ km s}^{-1} \text{ Mpc}^{-1}$. The magnitudes are given in the AB system.

2. Detectability of Kilonovae Associated with FRBs

Recently several authors have investigated spectra and light curves of kilonovae taking opacity of r -process elements into account (Barnes & Kasen 2013; Tanaka & Hotokezaka 2013; Grossman, Korobkin, Rosswog, & Piran 2014). Although the models of kilonovae are still uncertain, it is broadly agreed that the optical light curve rapidly decays within a few days after the explosion, while the NIR light curve gradually rises and peaks several days later.

In the left panel of figure 1, we show kilonova light curves predicted by Tanaka & Hotokezaka (2013) and Barnes & Kasen (2013) using fiducial parameter sets in their studies. The models are broadly consistent in their late time NIR light curves, while the light curves in the first couple of days after the explosion and/or in optical wavelengths are different from each other. Besides the model uncertainties, the luminosity of a kilonova largely depends on some parameters such as mass and velocity of the ejecta from the merging NS-NS binary. It is possible that kilonovae span a wide range of peak luminosities, although their luminosity function is not known. In the following discussion, we use the fiducial model of Tanaka & Hotokezaka (2013, hereafter TH13 model) to make a rough estimate of the feasibility of optical follow up observations.

The currently known FRBs are discovered by the multibeam receiver on the 64-m Parkes radio telescope (Staveley-Smith et al. 1996) and the Arecibo L-band Feed Array on the 305-m Arecibo telescope (Cordes et al. 2006). With these radio telescopes, the typical localization error radius of a FRB is several arcmin, which can be covered by wide-field cameras of 8m-class telescopes such as Suprime Cam/Hyper Suprime Cam (SCam/HSC) on Subaru.

The kilonova models predict that the light curves in shorter wavelength range decay earlier, and hence the optical follow up should be performed in red bands. With 8-m class telescopes, an i -band image with limiting magnitude ~ 27.5 ($S/N = 5$) can be achieved with 3–4 hours of exposure. In the right panel of figure 1, we show the observer frame i -band light curves of kilonovae at various redshifts predicted by the TH13 model. We may detect kilonovae at redshifts up to $z \sim 0.3$ if we perform an imaging down to $i \sim 27.5$ within ~ 3 days after FRBs. Hence FRBs with DM smaller than that corresponding to $z \sim 0.3$ will be good targets of the optical follow up observations. The expected peak NIR magnitude of a kilonova at $z \sim 0.3$ is $H \sim 26$. Hence it would be difficult to detect a kilonova at a cosmological distance with a ground based NIR telescope.

Assuming a constant FRB rate and the maximum observable redshift of FRBs to be $z = 1$, the FRB rate reported in Thornton et al. (2013) becomes $2.4_{-1.2}^{+1.4} \times 10^4 \text{ yr}^{-1} \text{ Gpc}^{-3}$. Then the event rates of $z < 0.3$ FRBs in the field of views of the Parkes multibeam receiver and the Arecibo L-band Feed Array (Staveley-Smith et al. 1996; Spitler et al. 2014) are $\sim 2.3 \text{ yr}^{-1}$ and $\sim 0.45 \text{ yr}^{-1}$, respectively.

We note that Hassall, Keane, & Fender (2013) showed that FRB rate estimates change by an order of magnitude depending on the treatment of the scattering of radio pulses as they propagate through a plasma. It is also likely that the FRB rate density depends on redshift as discussed in Totani (2013). The observed redshift evolution of the SN Ia rate density is expressed as $\propto (1+z)^2$ (Okumura et al. 2014). We expect that the redshift dependence of the rate density of NS-NS mergers would be similar to that of SN Ia, because the delay time distribution of NS-NS mergers is expected to be $\propto t^{-1}$ (Totani 1997; Dominik et al. 2013) and the same delay time distribution is also suggested for SNe Ia (Totani et al. 2008; Maoz, Mannucci, & Nelemans 2013).

3. Estimation of Contaminating SN Rate

When we search for an optical counterpart of a FRB, it is possible that physically unrelated SNe coincide within the positional error by chance. To investigate the population of SNe that contaminate the FRB follow up observations, we randomly generate a mock catalog of SNe in the field considering SN types Ia, Ibc, IIL, IIP, and IIIn at various redshifts.

Redshifts of the mock SNe are sampled at intervals of $\Delta z = 0.05$ up to $z = 2$ ($z = 4$ for IIIn) where the SNe become undetectable at the peak times by currently available facilities ($i > 27.5$). At each sampled redshift, we randomly generate 1000 sets of light curves in observer frame i and z -band for each of the SN types, considering peak time luminosity distribution of each SN type. When generating SN Ia light curves, we follow the method of Barbary et al. (2012) in which luminosity of a SN Ia correlates with its stretch and color. For core-collapse SNe (Ibc, IIL, IIP, and IIIn), we follow the method of Dahlen et al. (2012). Dust extinction in SN host galaxies are included in these models. Each light curve follows the templates of SN spectral evolutions provided by Hsiao et al. (2007) and Nugent, Kim, & Perlmutter (2002).

For each of the generated light curves, we consider various timings of the observation ranging -30–1000 days relative to the peak time of each SN sampled at intervals of 1 day. For each of the sampled timings, we obtain apparent i and z magnitudes and their later evolution. To simulate the SN population which we would find in the field, we integrate the mock SN sample over redshifts weighted with cosmic SN rate history of each SN type. We assume SN Ia rate history of Okumura et al. (2014), and core-collapse SN rates proportional to the cosmic star formation rate history (Behroozi, Wechsler, & Conroy 2013) normalized to core-collapse SN rates at $z < 1$ (Dahlen et al. 2012).

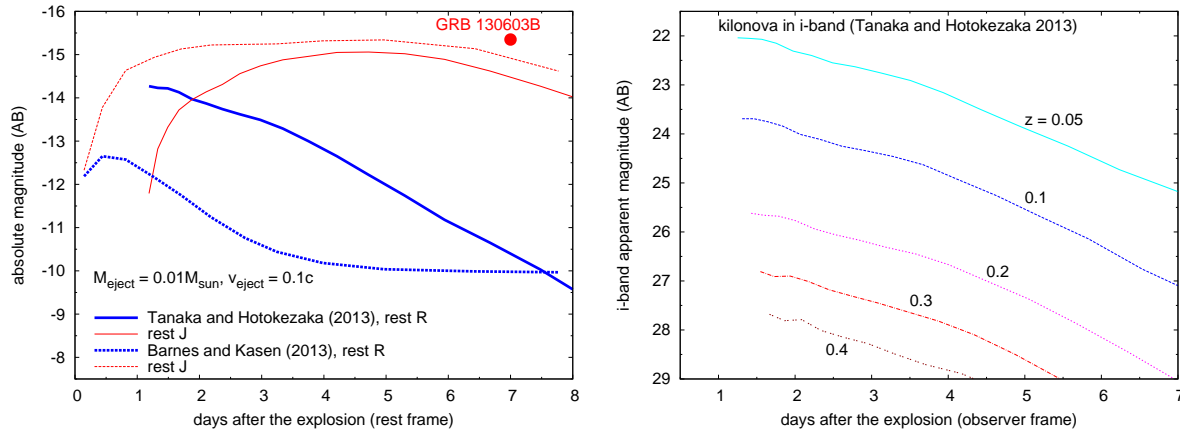


Fig. 1. Left panel: rest frame light curves of kilonovae in absolute magnitude predicted by the models of Tanaka & Hotokezaka (2013, TH13) and Barnes & Kasen (2013). The thick and thin lines represent the light curves in rest frame R -band and J -band, respectively. The circle at the top right indicates observing time and luminosity of the kilonova candidate associated with GRB 130603B ($z = 0.356$) in HST F160W filter which roughly corresponds to rest frame J -band. Right panel: apparent light curves in observer frame i -band predicted by the TH13 model at different redshifts.

We consider a case that we take a residual of 2 images taken with a certain time interval to find transient events. The interval of several days would be sufficient to find a kilonova due to their rapid decay. We note that, when a transient is embedded on a background object such as its host galaxy and we cannot separate them, the flux information we can obtain is limited to $f_{\nu,1st} - f_{\nu,2nd}$, where $f_{\nu,1st}$ and $f_{\nu,2nd}$ are the fluxes of the transient in the first and the second image. In this case, we need another (third) image with a sufficient time interval as a reference frame that does not include light from the transient, to measure the total (i.e., non-residual) flux of the transient, $f_{\nu,1st}$ and $f_{\nu,2nd}$, separately.

In figure 2, we show distribution of i -band magnitudes of each SN type in the first and second image (i_{1st} and i_{2nd}) taken with the intervals of 5 days. SNe are distributed along the $i_{1st} = i_{2nd}$ line, although a few SNe are in rapidly rising phase ($i_{1st} > i_{2nd}$). When the interval is shorter the scatter of the SN distribution around the $i_{1st} = i_{2nd}$ line is smaller (< 0.1 mag in the case of the 1 day interval).

4. Distinguishing a FRB and SNE

In figure 3, we show distributions of total i -band magnitudes of SNe and those in the residual images with the intervals of 5 days and 1 day predicted by the mock SN catalog. The magnitude in the residual image (m_{res}) can be expressed as $m_{res} = -2.5 \log_{10} |f_{\nu,1st} - f_{\nu,2nd}| - 48.6$, where $f_{\nu,1st}$ and $f_{\nu,2nd}$ are in a unit of $\text{erg s}^{-1} \text{cm}^{-2} \text{Hz}^{-1}$. The i_{res} distribution of rising and decaying SNe are plotted separately in figure 3. When we search for a kilonova in the field, we consider only decaying SNe as contaminants. Although i_{res} of SNe are significantly fainter than their total magnitudes, we would detect some contaminants in a deep survey. In a survey down to the depth of $i_{res} = 27.5$, the number density of contaminants is 73.5 deg^{-2} with the interval of 5 days (i.e. 1.6 SNe within an

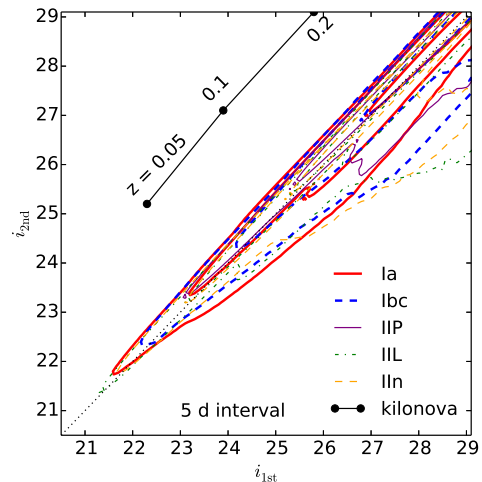


Fig. 2. Distribution of SNe on the i_{1st} vs. i_{2nd} plane with the interval of 5 days. The contours indicate number density of the SNe on this plane of 1, 10, and 100 $\text{mag}^{-2} \text{deg}^{-2}$. The 5 SN types considered in our SN model (Ia, Ibc, IIL, IIP, and IIc) are plotted separately. Kilonovae at different redshifts are plotted together with the first observation at 2 days after the explosion. The dotted line indicates $i_{1st} = i_{2nd}$.

error radius of 5 arcmin). The number density of contaminants is smaller with the 1 day interval. However, kilonovae decay only by $\sim 50\%$ of their luminosity within the 1 day interval, and i_{res} of kilonovae would also become significantly fainter than the total magnitudes making kilonova detection more difficult.

Tanaka & Hotokezaka (2013) showed that kilonovae have redder color than SNe throughout their evolution. However, it should be noted that SNe may have similar apparent color to kilonovae, when reddened by dust or cosmologically redshifted. One clue to distinguish kilonovae from SNe is the color evolution. Color of a kilonova

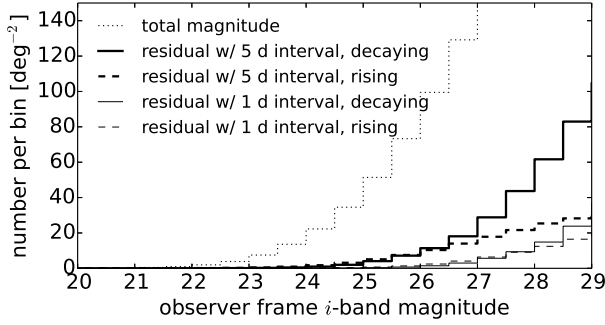


Fig. 3. Differential distributions of i -band magnitudes of contaminating SNe (all types). The dotted histogram represents the total magnitudes, while the other histograms represent those in the residual images with the intervals of 5 days and 1 day (thick and thin histograms, respectively). For the residual magnitudes, the solid and dashed lines represent the decaying and rising SNe, respectively.

changes by $\Delta(i-z) \gtrsim 1$ in the first several days after the explosion, while SN colors do not significantly change in such a timescale (the top panel of figure 4). Here we consider a case of a FRB follow-up starting at 2 days after the explosion, followed by the second optical observation with an interval of 1 or 5 days from the first. The large color evolution of $\Delta(i-z) \gtrsim 1$ can be realized over photometric errors when kilonovae are detected with $S/N > 5$, although detection in the second image may be available only for kilonovae at $z \lesssim 0.1$ and/or brighter events than considered here.

Another clue to distinguish kilonovae from SNe is the rapid decay of kilonovae in optical wavelengths as shown in figure 2. In the bottom panel figure 4, we show distribution of the fractional variability, $\Delta f/f = (f_{\nu,1st} - f_{\nu,2nd})/f_{\nu,1st}$, in i -band for decaying SNe with $i_{res} < 27.5$. SNe have $\Delta f/f \lesssim 0.3$ (0.1), while a kilonova reduces its flux by $\Delta f/f \gtrsim 0.9$ (0.3) during the 5 days (1 day) interval. The fractional variability can be used to distinguish a kilonova from SNe, even when the kilonova is not detected in the second image. If we perform i -band imaging of a kilonova at $z = 0.3$ at 2 days and 7 days after the explosion with the limiting magnitude of $i = 27.5$, the magnitude and the limit which we obtain in the two images would be $i_{1st} = 27.0$ and $i_{2nd} > 27.5$, respectively (the right panel of figure 1). In this case, we obtain a limit of $\Delta f/f > 0.37$ which is sufficient to distinguish the kilonova from SNe. Thus it is possible to distinguish kilonovae with i -band magnitudes down to $i_{1st} \sim 27$ (i.e 0.5 mag above the limit).

It is also possible that active galactic nuclei (AGNs) and/or galactic variables contaminate the follow up observations. However, AGNs with variability timescale $\lesssim 10$ days are rare (e.g. Totani et al. 2005; Morokuma et al. 2008). Furthermore, AGNs would always appear at the center of their host galaxies, while kilonovae have wide variety of offsets from the center as suggested from observations of short GRBs (1–50 kpc, Fong, Berger, & Fox 2010). The number density of galactic variables are also smaller than that of SNe at high galactic latitudes ($\sim 1/4$,

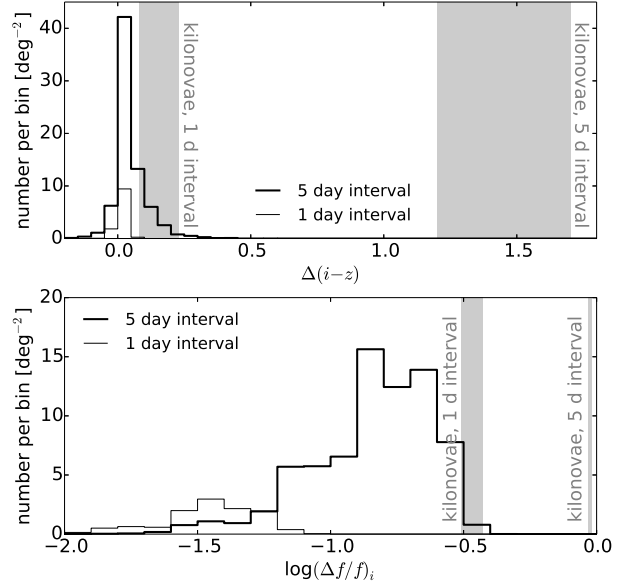


Fig. 4. Distributions of the color evolution of SNe [$\Delta(i-z)$, top panel] and the fractional variability flux in i -band ($\Delta f/f$, bottom panel), with the time intervals of 5 days and 1 day. Only decaying SNe with $i_{res} < 27.5$ are considered. The lines are the same as those in figure 3. The shaded regions indicate $\Delta(i-z)$ and $\Delta f/f$ of kilonovae at $z \leq 0.3$ with the first observation at 2 days after the explosion.

Morokuma et al. 2008), We also note that galactic variables typically have $\Delta f/f \lesssim 0.3$ in i -band (e.g. Ivezić et al. 2000), and would not be associated with a candidate host galaxy in most cases. Thus it would not be difficult to distinguish a kilonova from AGNs and galactic variables.

5. Discussion

We have investigated the detectability of FRB optical counterparts in the scenario that FRBs originate from NS-NS mergers as proposed by Totani (2013). NS-NS mergers may accompany radioactive emissions called kilonovae. Although the recent models of kilonovae are still highly uncertain, they suggest that a kilonova may be detectable at a cosmological distance if we perform a deep imaging (e.g. down to $i \sim 27.5$) within a few days. However, we also expect to find a few unrelated SNe within an error region of a FRB.

We have compared the light curve and the color evolution of a kilonova predicted by the TH13 model to those of SN templates at various redshifts, and found that kilonovae can be distinguished from SNe by the color evolution [e.g. $\Delta(i-z)$] and/or the fractional variability ($\Delta f/f$). If real-time alerts of FRBs become available in near future, we suggest to perform deep imagings of positions of FRBs suggested to be at low redshifts (e.g. $z \lesssim 0.3$) from their DMs in red optical bands, starting within a couple of days and with intervals of several days. With an interval of 5 days and limiting magnitudes of $i = 27.5$, it would be possible to distinguish a kilonova with i -band magnitudes down to $i_{1st} \sim 27$.

It should be noted that we have implicitly assumed that every NS-NS merger accompanies kilonova. Although a kilonova candidate is found associated with a short GRB 130603B (Tanvir et al. 2013; Berger, Fong, & Chornock 2013), it is possible that NS-NS mergers which cause GRBs tend to eject more mass, producing brighter kilonovae. If other NS-NS mergers than the progenitor of GRB 130603B typically produce fainter (or no) kilonovae, we may find no optical counterpart even if FRBs originate from NS-NS mergers.

The FRB rate is consistent with that of NS-NS mergers, but at the high end of the plausible range (Totani 2013; Hassall, Keane, & Fender 2013), suggesting that almost all NS-NS mergers produce FRBs. Kilonovae is an important candidate of the production site of r -process elements in the universe. Searches for kilonovae associated with FRBs may enable us to investigate what fraction of NS-NS mergers produce kilonovae, and to constrain the cosmic history of r -process element production.

If the kilonova rate is close to the FRB rate reported by Thornton et al. (2013), a blind search of kilonovae with a wide field optical camera is also interesting. When we take an image with a limiting magnitude of $i = 27.5$, similarly to the case of the FRB follow up observations discussed here, the expected number of kilonovae is 0.03 ± 0.02 per 1 deg^2 , assuming the same FRB rate at $z < 0.3$ as in Section 2.

In the case that FRBs originates from WD-WD mergers, it is possible that they accompany SNe Ia as their optical counterparts, although the association of SNe Ia with WD-WD mergers remains a matter of debate. A SN Ia can be detected up to higher redshifts in the FRB follow up observations discussed above (up to $z \sim 0.9$ when observed down to $i_{\text{res}} \sim 27.5$ at 2 and 7 days after the explosion), and one can also search it around the expected peak time of the SN Ia (i.e. ~ 20 days after the FRB in the rest frame).

Since light curves of SNe Ia are well studied (e.g. Hsiao et al. 2007), if a SN Ia is spectroscopically confirmed and several data points of its light curve are obtained in an error region of a FRB, it would be possible to constrain the explosion time with a day scale precision. SNe with $i < 24.0$ can be spectroscopically classified using 8m-class telescopes, and the expected number density of unrelated SNe with $i < 24.0$ is 28.8 deg^{-2} (i.e. 0.63 SNe within an error radius of 5 arcmin , figure 3). For SNe Ia, the magnitude limit of $i < 24.0$ corresponds to $z \lesssim 0.6$. When we follow up a FRB whose DM corresponds to $z < 0.6$, the expected rate of unrelated SNe Ia at $z < 0.6$ within an error radius of 5 arcmin is $< 0.003 \text{ day}^{-1}$, assuming cosmic SN Ia rate density at $z < 0.6$ to be $< 5 \times 10^{-5} \text{ yr}^{-1} \text{ Mpc}^{-3}$ (e.g. Okumura et al. 2014). Thus, if we find a SN Ia in an error region of a FRB with consistent explosion time, we would be able to conclude that the SN Ia is the counterpart of the FRB with a significant confidence level.

We are grateful to the anonymous referee for helpful comments. Y.N. is supported by the Research Fellowship for Young Scientists from the Japan Society for the Promotion of Science (JSPS).

References

- Bannister, K. W., & Madsen, G. J. 2014, MNRAS, 440, 353
 Barbary, K., Aldering, G., Amanullah, R., et al. 2012, ApJ, 745, 31
 Barnes, J., & Kasen, D. 2013, ApJ, 775, 18
 Behroozi, P. S., Wechsler, R. H., & Conroy, C. 2013, ApJ, 770, 57
 Berger, E., Fong, W., & Chornock, R. 2013, ApJL, 774, L23
 Burke-Spolaor, S., Bailes, M., Ekers, R., Macquart, J.-P., & Crawford, F., III 2011, ApJ, 727, 18
 Cordes, J. M., Freire, P. C. C., Lorimer, D. R., et al. 2006, ApJ, 637, 446
 Dahlen, T., Strolger, L.-G., Riess, A. G., et al. 2012, ApJ, 757, 70
 Dennison, B. 2014, MNRAS, 443, L11
 Dominik, M., Belczynski, K., Fryer, C., et al. 2013, ApJ, 779, 72
 Falcke, H., & Rezzolla, L. 2014, A&A, 562, A137
 Fong, W., Berger, E., & Fox, D. B. 2010, ApJ, 708, 9
 Grossman, D., Korobkin, O., Rosswog, S., & Piran, T. 2014, MNRAS, 439, 757
 Hassall, T. E., Keane, E. F., & Fender, R. P. 2013, MNRAS, 436, 371
 Hsiao, E. Y., Conley, A., Howell, D. A., et al. 2007, ApJ, 663, 1187
 Ivezić, Ž., Goldston, J., Finlator, K., et al. 2000, AJ, 120, 963
 Kashiyama, K., Ioka, K., & Mészáros, P. 2013, ApJL, 776, L39
 Keane, E. F., Stappers, B. W., Kramer, M., & Lyne, A. G. 2012, MNRAS, 425, L71
 Kulkarni, S. R., Ofek, E. O., Neill, J. D., Zheng, Z., & Juric, M. 2014, arXiv:1402.4766
 Li, L.-X., & Paczyński, B. 1998, ApJL, 507, L59
 Loeb, A., Shvartzvald, Y., & Maoz, D. 2014, MNRAS, 439, L46
 Lorimer, D. R., Bailes, M., McLaughlin, M. A., Narkevic, D. J., & Crawford, F. 2007, Science, 318, 777
 Maoz, D., Mannucci, F., & Nelemans, G. 2013, arXiv:1312.0628
 Morokuma, T., Doi, M., Yasuda, N., et al. 2008, ApJ, 676, 163
 Nugent, P., Kim, A., & Perlmutter, S. 2002, PASP, 114, 803
 Okumura, J. E., Ihara, Y., Doi, M., et al. 2014, arXiv:1401.7701
 Popov, S. B., & Postnov, K. A. 2013, arXiv:1307.4924
 Spitler, L. G., Cordes, J. M., Hessels, J. W. T., et al. 2014, arXiv:1404.2934
 Staveley-Smith, L., Wilson, W. E., Bird, T. S., et al. 1996, PASA, 13, 243
 Tanaka, M., & Hotokezaka, K. 2013, ApJ, 775, 113
 Tanvir, N. R., Levan, A. J., Fruchter, A. S., et al. 2013, Nature, 500, 547
 Thornton, D., Stappers, B., Bailes, M., et al. 2013, Science, 341, 53
 Totani, T. 2013, PASJ, 65, L12
 Totani, T. 1997, ApJL, 486, L71
 Totani, T., Morokuma, T., Oda, T., Doi, M., & Yasuda, N. 2008, PASJ, 60, 1327
 Totani, T., Sumi, T., Kosugi, G., et al. 2005, ApJL, 621, L9
 Tuntsov, A. V. 2014, MNRAS, 441, L26
 Yi, S.-X., Gao, H., & Zhang, B. 2014, arXiv:1407.0348
 Zhang, B. 2014, ApJL, 780, L21